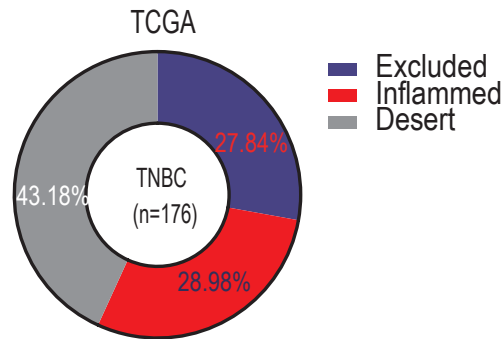
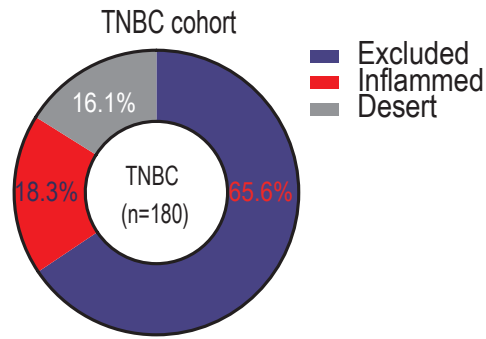
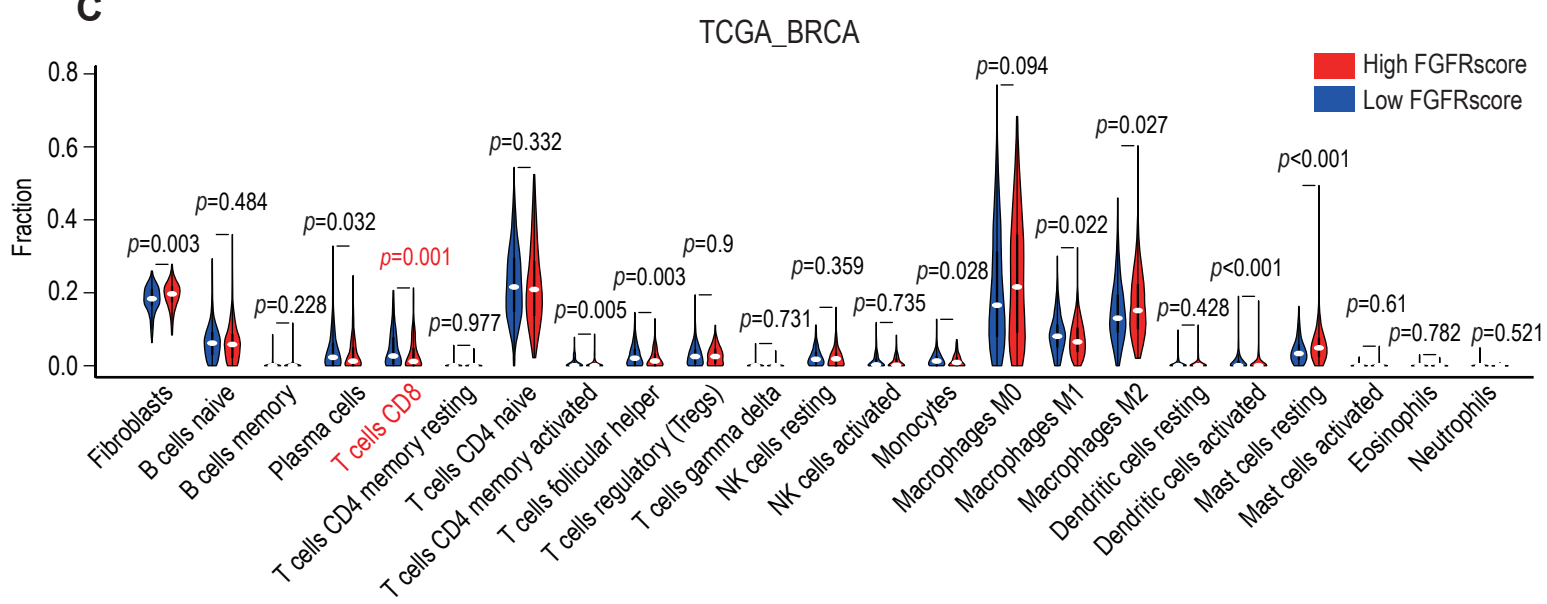
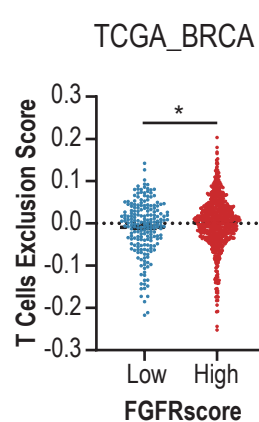
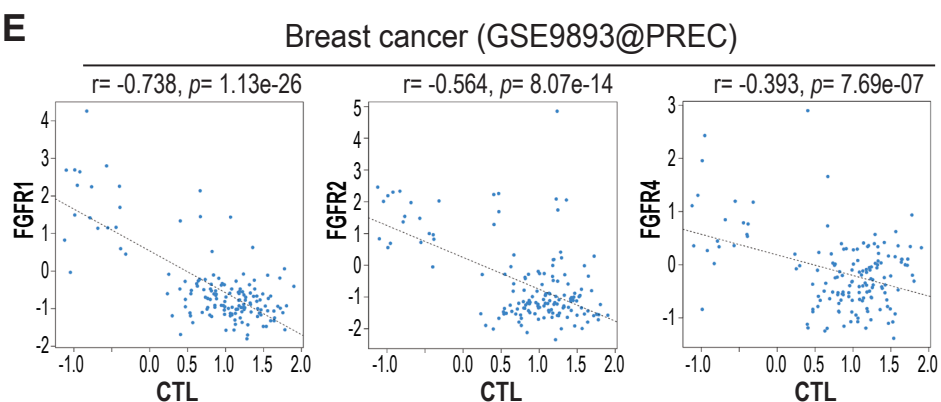
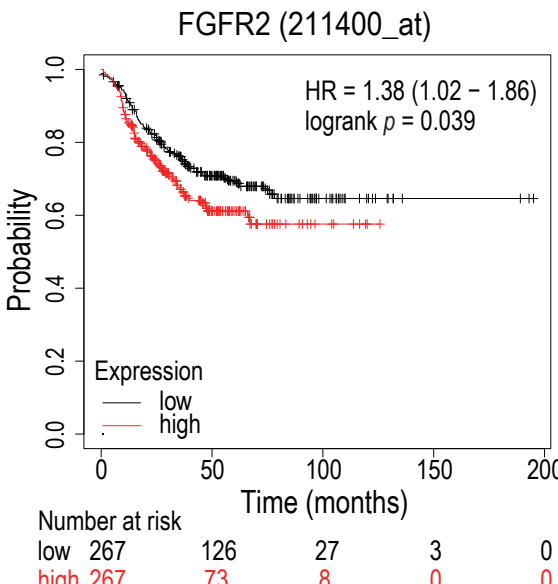
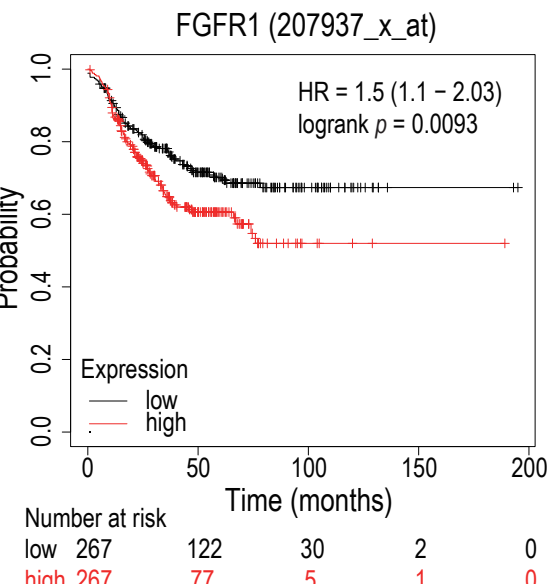
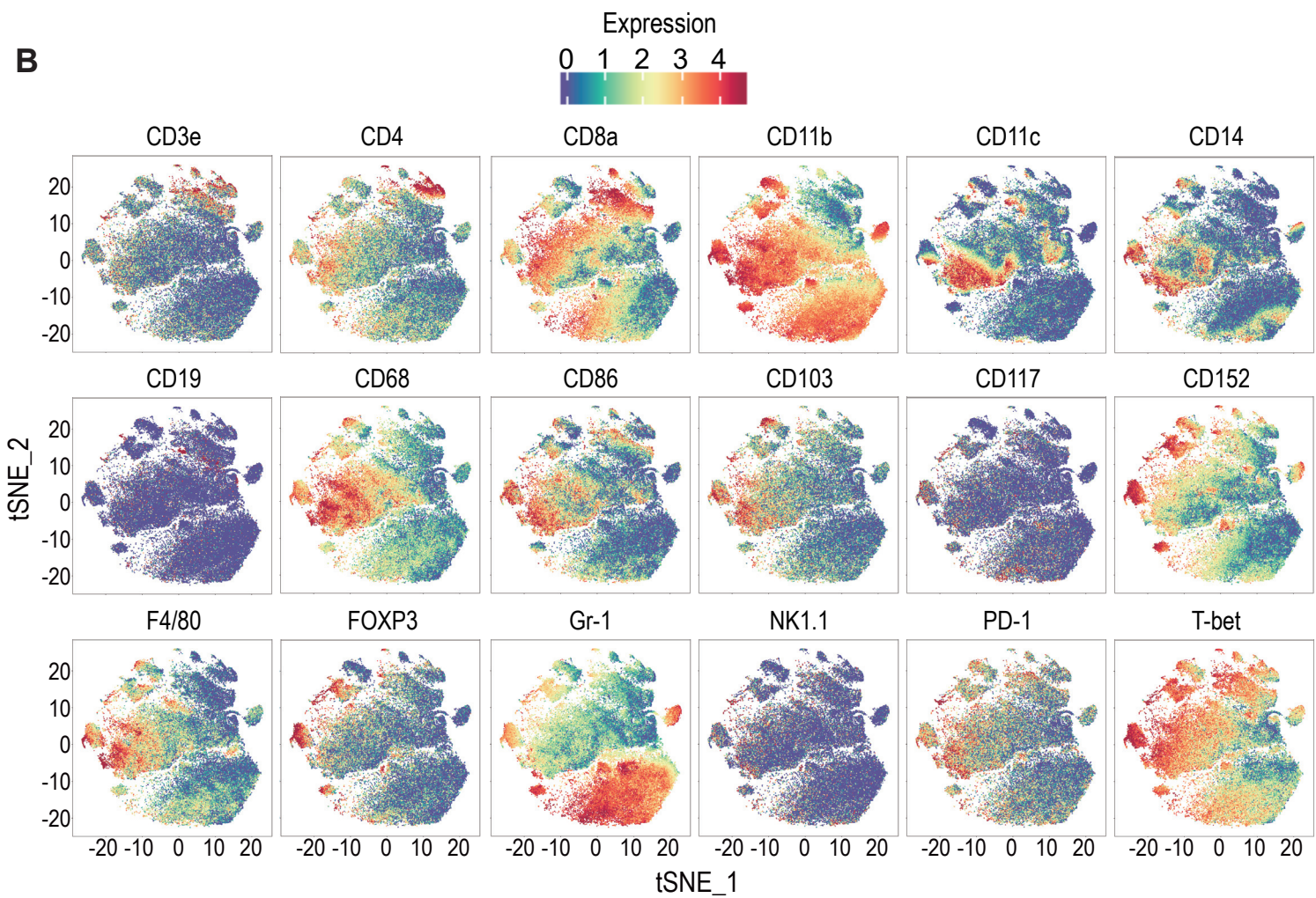
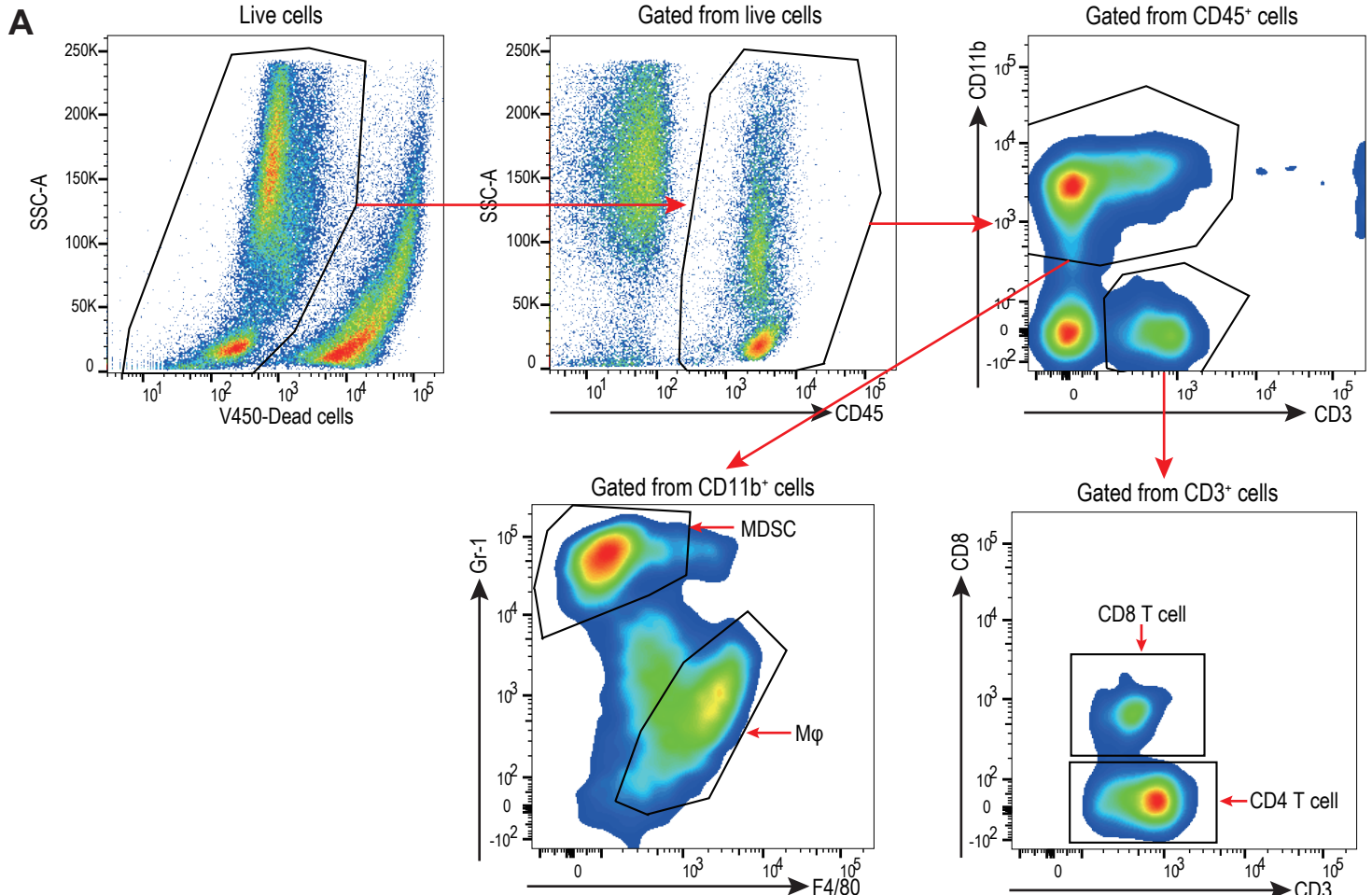
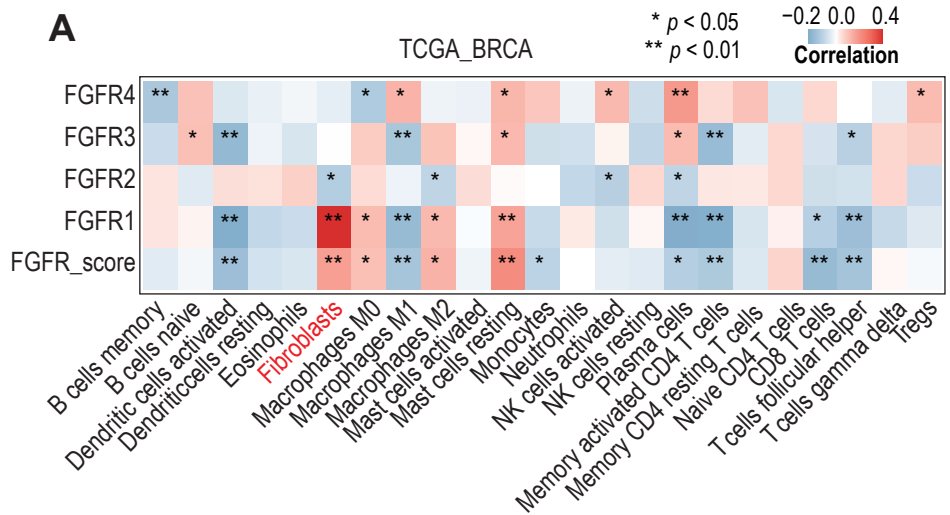
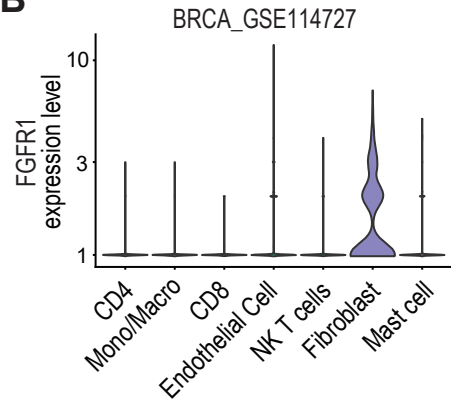
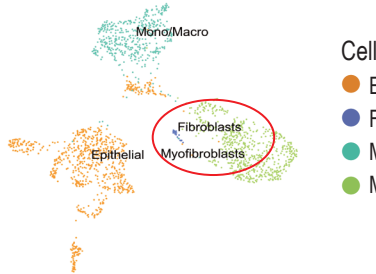


**A****B****C****D****E****F**

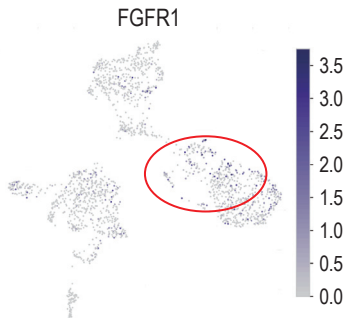


**A****B****C**

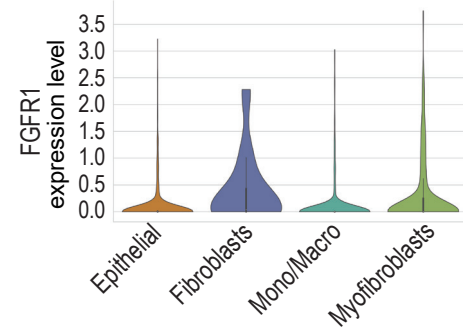
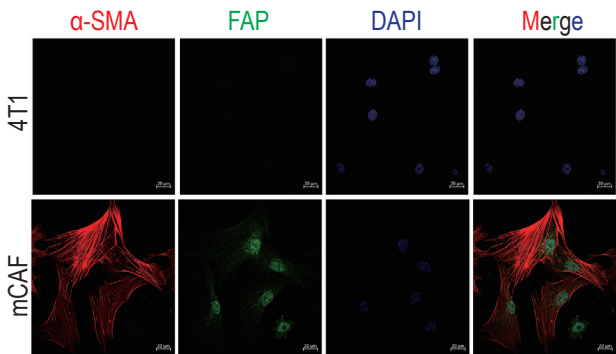
BRCA\_GSE138536

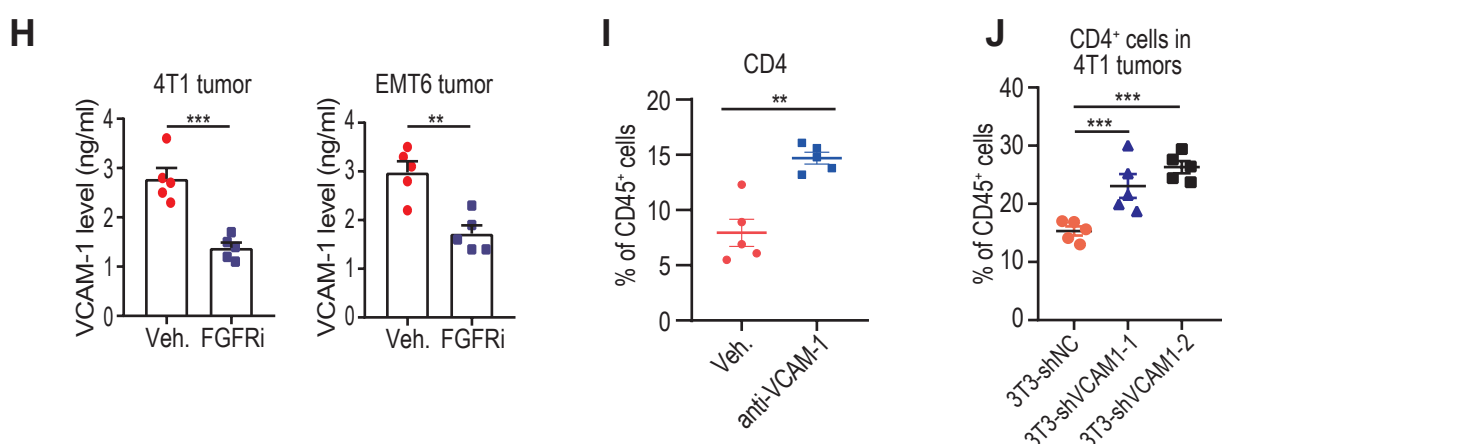
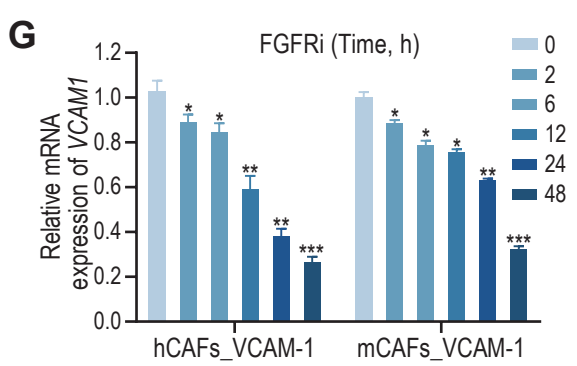
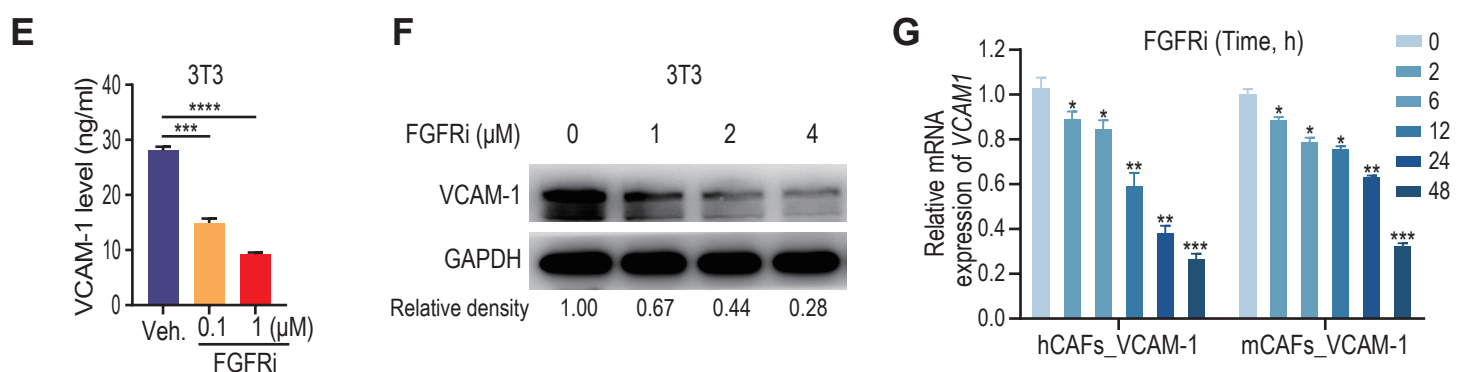
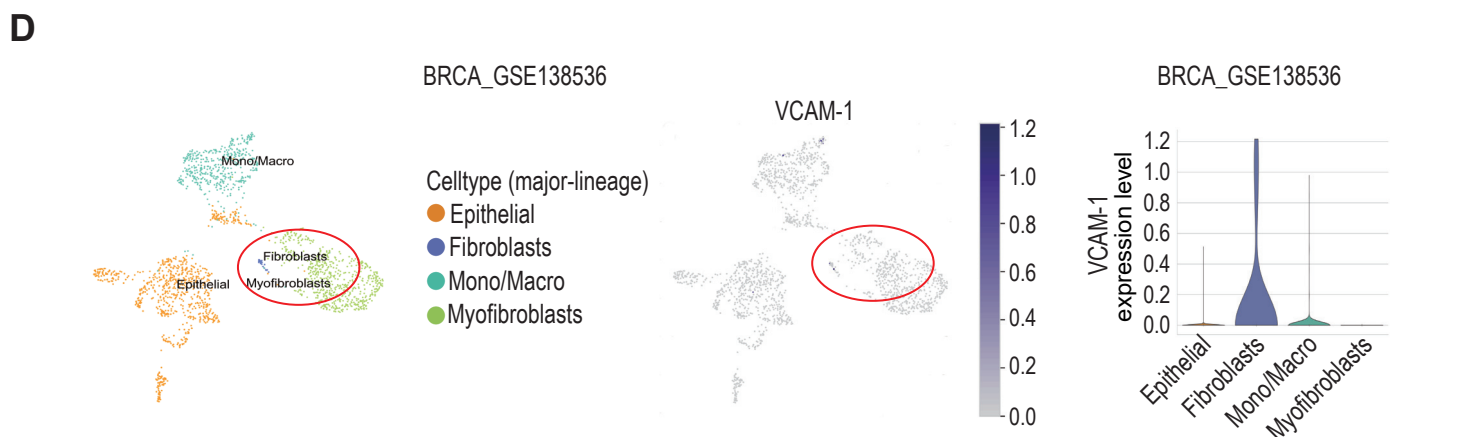
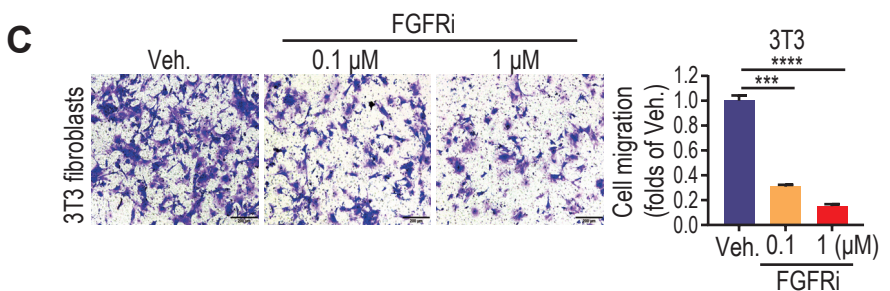
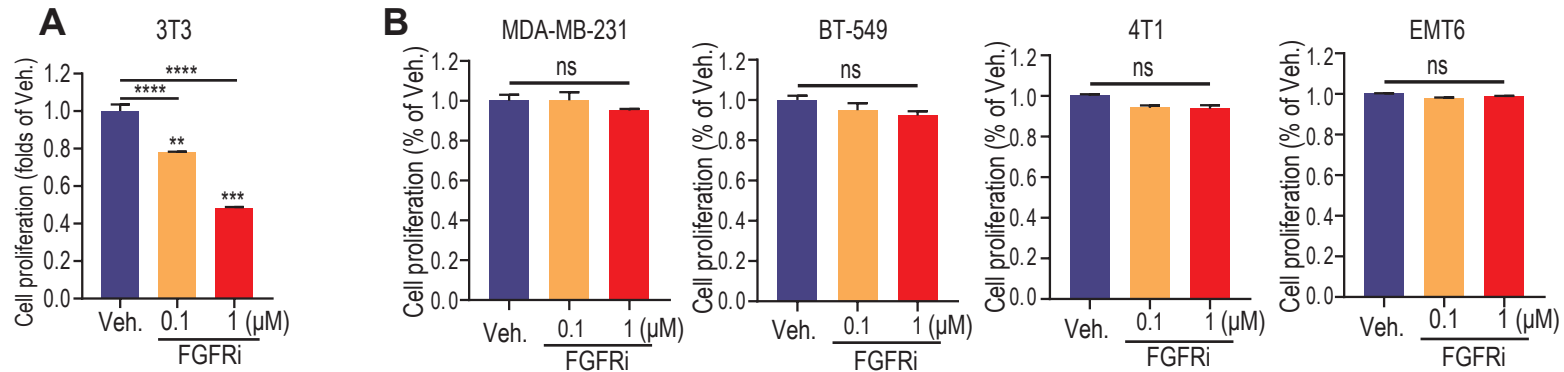


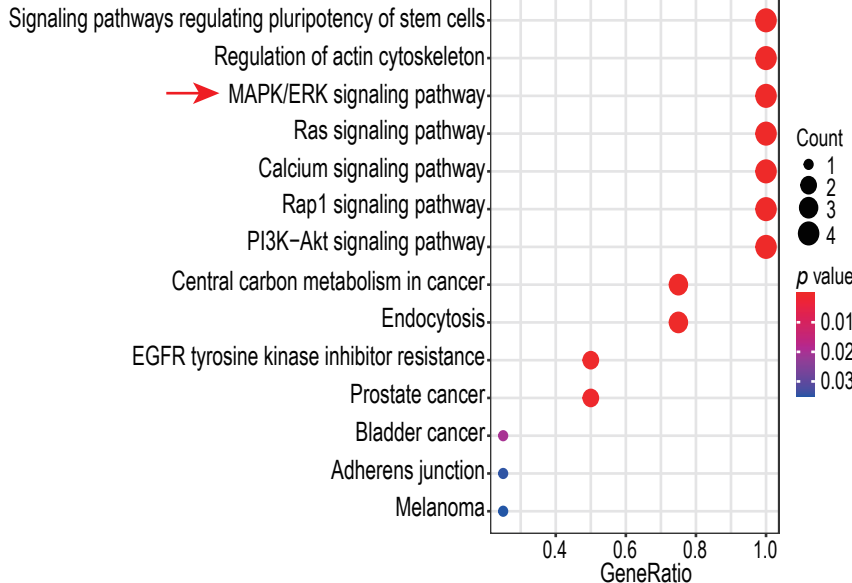
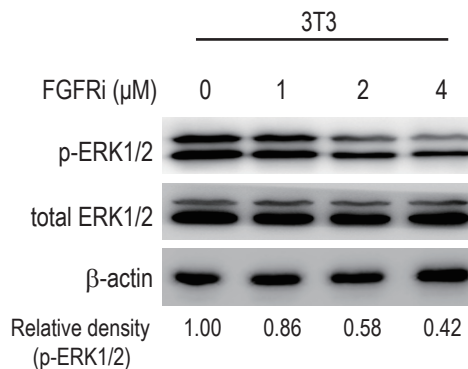
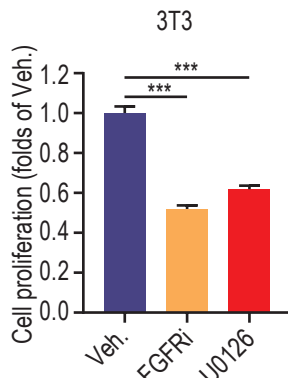
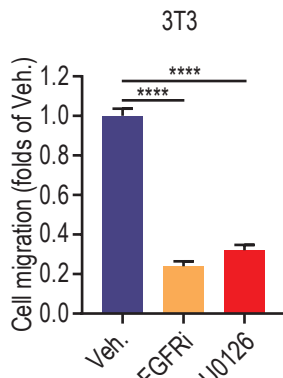
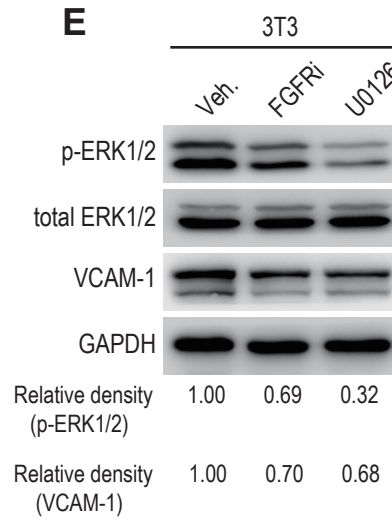
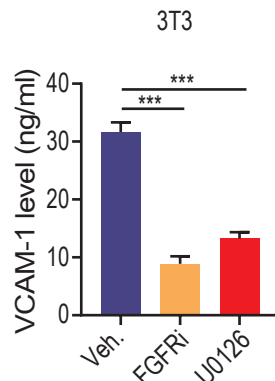
- Celltype (major-lineage)
- Epithelial
  - Fibroblasts
  - Mono/Macro
  - Myofibroblasts

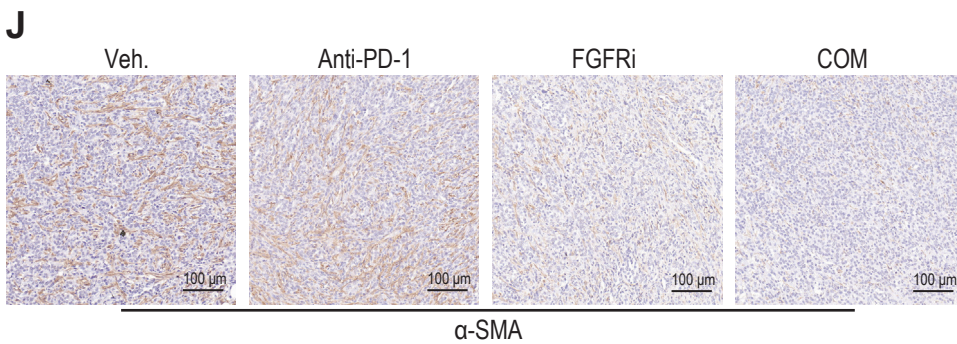
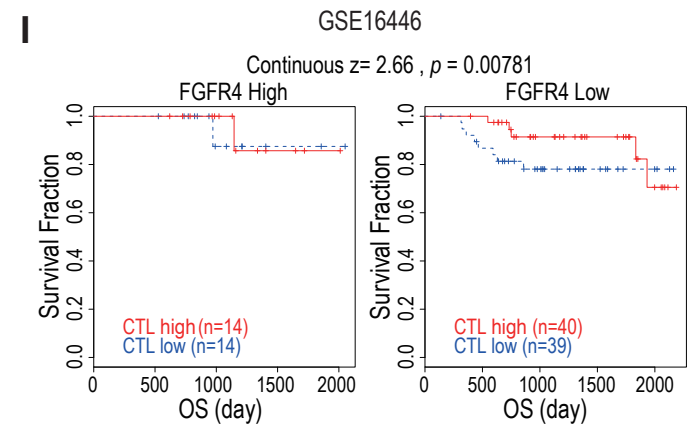
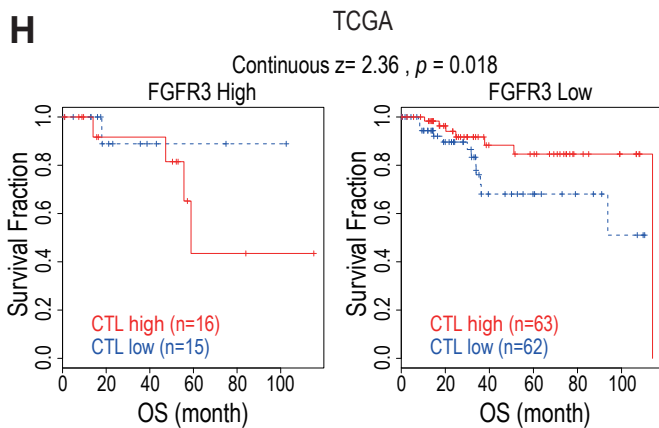
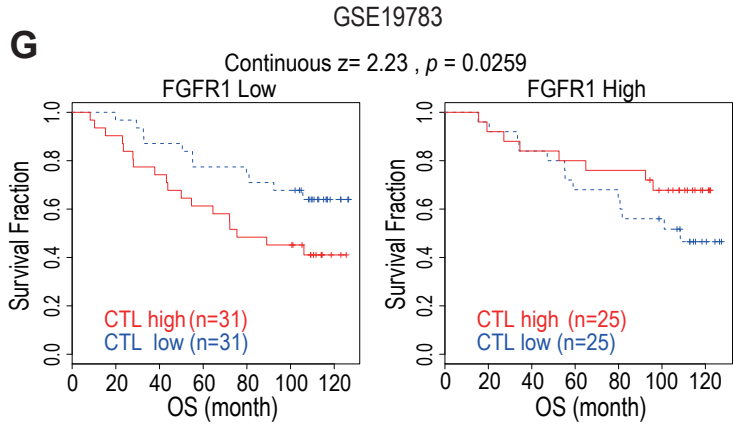
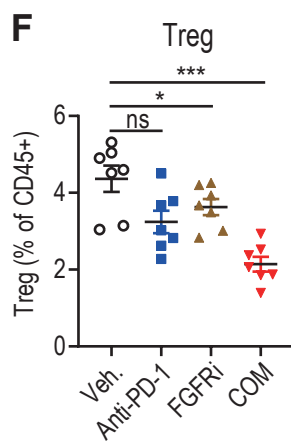
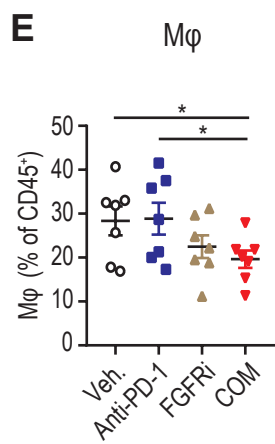
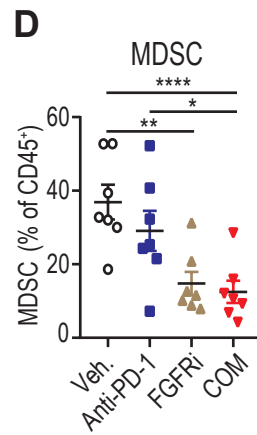
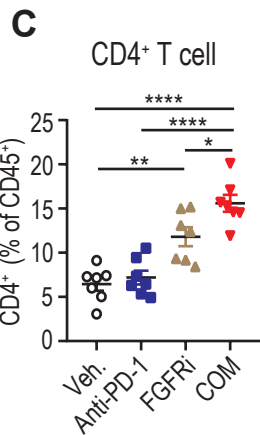
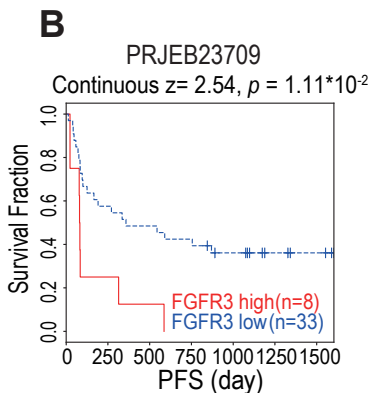
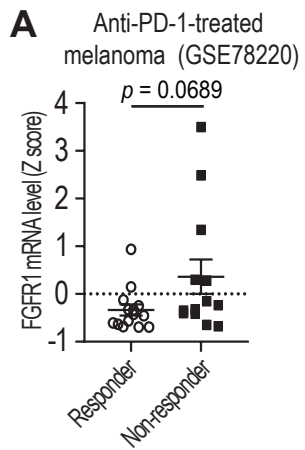


BRCA\_GSE138536

**D**



**A****B****C****D****E****F**



## **Supplementary Figure legends**

**Figure S1.** The correlation between FGFR1/2 expression and relapse-free survival (RFS) of patients with TNBC. A) Immune phenotypes of TNBC from TCGA database. B) Immune phenotypes of our TNBC cohort. C) Differences in 23 types of stromal cells from TME in BRCA of TCGA were compared after grouping by median FGFRscore. D) Differences in T cell exclusion score in BRCA of TCGA were compared after grouping by median FGFRscore. E) The correlation between FGFR1/2/4 expression and cytotoxic T lymphocytes (CTL) infiltration in breast cancer (GSE9893 dataset) based on Tumor Immune Dysfunction and Exclusion (TIDE) system. F) The correlation between FGFR1/2 expression and relapse-free survival (RFS) of patients with TNBC from Kaplan-Meier (KM) Plotter database.

**Figure S2.** tSNE plot of TILs overlaid with the expression of indicated markers. A) Gating strategy to identify immune cell subsets in 4T1 tumor. B) tSNE plot of TILs overlaid with the expression of indicated markers.

**Figure S3.** FGFR1 expression in tumor microenvironment of breast cancer. A) The correlation between FGFRs and 23 types of stromal cells from TME in BRCA of TCGA. B) FGFR1 expression in TME of breast cancer (GSE114727). C) FGFR1 expression in TME of breast cancer from GSE138536 dataset. D) Representative images of  $\alpha$ -SMA and FAP immunofluorescent staining in 4T1 cells and mouse CAFs.

**Figure S4.** Blocking FGFR pathway inhibited cell proliferation, migration and VCAM-1 secretion of CAFs. A) The effect of FGFRi Erdafitinib on cell proliferation of 3T3 fibroblasts for 48 h was detected by CCK-8 assay (n=3 biological replicates, one-way ANOVA). B) The effect of FGFRi Erdafitinib on cell proliferation of breast cancer cell lines for 48 h was detected by CCK-8 assay. C) The effect of FGFRi Erdafitinib on cell migration of 3T3 fibroblasts was detected by transwell migration assay (n=3 biological replicates, one-way ANOVA). D) VCAM-1 expression in TME of breast cancer from GSE138536 dataset based on TISCH system. E) The effect of FGFRi Erdafitinib on VCAM-1 level in cell supernatant of 3T3 fibroblasts was detected by ELISA (n=3 biological replicates, one-way ANOVA). F) The effect of FGFRi Erdafitinib on VCAM-1 expression of 3T3 fibroblasts was detected by western blot. G) The effect of different durations of FGFRi Erdafitinib on VCAM-1 mRNA expression in human CAFs and mouse CAFs was examined by qPCR. H) The effect of FGFRi Erdafitinib on VCAM-1 level in tumor extract of 4T1 and EMT6 tumors was detected by ELISA (n=3 biological replicates, one-way ANOVA). I) CD4<sup>+</sup> T cell population in primary 4T1 tumors from mice treated with vehicle or anti-VCAM1 (n=5, one-way ANOVA). J) Percentages of CD4<sup>+</sup> T cells in primary 4T1 tumors from mice treated with indicated therapies (n=5, one-way ANOVA).

**Figure S5.** The activation of MAPK/ERK pathway maintains FGFRs function in CAFs *in vitro*. A) GSEA (Reactome pathway analysis) of FGFR1-4 in breast cancer from GEO. B) The effect of FGFRi Erdafitinib on p-ERK1/2 and total ERK1/2 expression of 3T3 fibroblasts was detected by western blot. C) The effect of MAPK pathway inhibitor U0126 on cell proliferation of and 3T3 fibroblasts for 48 h was detected by CCK-8 assay (n=3 biological replicates, one-way ANOVA). D) The effect of U0126 on cell migration of 3T3 fibroblasts was detected by transwell migration assay (n=3 biological replicates, one-way ANOVA). E) The effect of U0126 on VCAM-1 expression of 3T3 fibroblasts was detected by western blot. F) The effect of U0126 on VCAM-1 level in cell supernatant of 3T3 fibroblasts was detected by ELISA (n=3 biological replicates, one-way ANOVA).

**Figure S6.** High expression of FGFRs is correlated with poor survival of ICT-treated patients and T cell dysfunction. A) FGFR1 mRNA expression in pre-treatment tumors of responder (n=14) *versus* non-responder (n=13) melanoma patients (t-test). B) Progression-free survival of melanoma patients who had high FGFR3 *versus* low FGFR3 expressed in the tumors before anti-PD-1 treatment (PRJEB23709). C-F) Percentages of CD4<sup>+</sup> T cells, CD8<sup>+</sup> T cells, MDSC and Mφ in primary 4T1 tumors from mice treated with indicated therapies (n=6, one-way ANOVA). G-I) Kaplan-Meier survival analysis of low CTL (blue) *versus* high CTL (red) in FGFRs-high or FGFRs-low breast cancer. J) Representative α-SMA staining in indicated therapy-treated 4T1 tumors.